Effect of Scratch Velocity on Scratch Behavior of Injection-Molded Polypropylene

Vadee Chivatanasoontorn, Naoya Aoki, Masaya Kotaki

Department of Advanced Fibro-Science, Kyoto Institute of Technology, Sakyo-ku, Kyoto 606-8585, Japan

Received 22 July 2011; accepted 3 November 2011
DOI 10.1002/app.36432
Published online 31 January 2012 in Wiley Online Library (wileyonlinelibrary.com).

ABSTRACT: Scratch tests of polypropylene injection moldings were conducted with a progressive load scratch test according to ISO 19252. Effect of scratch velocity on scratch visibility and damage initiation was investigated. The results showed that the critical normal load for onset of scratch visibility was independent of scratch velocity in the range from 1 to 10 mm/s. However, the critical normal load decreased with increase of scratch velocity higher than 10 mm/s. The other scratch damage transitions such as onset of fish-scale and cutting pattern, the critical normal load also decreased with increase of scratch velocity. A correlation between scratch behavior and subsurface deformation was observed by polarized optical microscope. The formation of yielded zone under scratch groove was clearly observed at onset of scratch visibility. It was found that the yielded zone size becomes shallower at higher scratch velocity. The results suggested that localized stress was generated near the surface at higher scratch velocity.
 J Appl Polym Sci 125: 2861–2866, 2012

Key words: injection molding; polypropylene; scratch behavior; yielding; velocity

INTRODUCTION

The scratch behavior of polymer materials has drawn significant attention, because polymers are widely used in various kinds of applications such as electric products, optical lens, household products, and automotive interior where durability of surface quality is demanded.[1–3]

Polypropylene (PP) is one of the commodity plastics that can be used in many applications because of its good balance of low cost and superior properties.[3,4] However, visible scratch damages are easily formed in PP due to stress whitening. The fracture mechanism that can lead to stress whitening are crazing, voiding, and cracking.[1–7] The microfracture alters the light reflection on the surface and causes a visible damage detected by necked eyes.

Over the years, a variety of testing methods to evaluate scratch behavior of ceramic materials and polymeric materials have been proposed such as Mohs' mineral hardness test,[8,9] pencil load scratch test,[10,11] and Ford-five-finger scratch test.[12,13] All of these scratch test methods are conducted under constant load. Quantitative scratch properties cannot be obtained by these test methods or are difficult to be obtained. A new scratch test method has been recently developed by Sue and coworkers.[14,15] The test method is based on a progressive load. This method was standardized in ASTM D7027-5[16] and recently ISO 19252.[17] It was reported that various kinds of scratch damage transitions can be observed through a single scratch test[18–20] and scratch properties can be quantitatively evaluated by critical load for onset of scratch visibility. The different characterization methods have been used to evaluate the scratch damage mode such as scanning electron microscopy (SEM), atomic force microscopy (AFM), polarized optical microscopy (POM), and so on.[21–24] However, the scratch behavior of polymers is complex and depends on various parameters. Briscoe et al.[25–30] have studied factors for the scratch behavior, i.e. shape of scratch tip, applied normal load, testing temperature, interfacial lubrication, and sliding velocity. Browning et al.[19] studied the effect of ethylene content of the elastomer in soft thermoplastic olefins (TPOs) phase and testing rate on the scratch properties. They found that the scratch behavior of soft TPOs is more rate-dependent than rigid TPOs. Onset of visibility was observed at lower normal load and scratch depth decreased when the scratch testing rate increased. According to ASTM D7027-5 and ISO 19252, a constant scratch rate of 100 $\pm$ 0.5 mm/s is recommended. However, slower scratch velocities were used in many reports published in open literatures although scratch behavior might be affected by scratch velocity since the deformation behavior of polymers is rate dependent. The objective of this research work is to investigate the effect of scratch velocity on scratch behavior of injection-molded PP and to understand the scratch mechanism.

Correspondence to: M. Kotaki (m-kotaki@kit.ac.jp).

TABLE I
Characteristics of Injection-Molded PP Samples

Samples	Weigh average molecular weight (M_w)	MFR (g/10 min)	Tensile modulus (GPa)	Tensile yield strength (MPa)
PP-a	190,000	21	1.6	35
PP-b	250,000	11	1.7	36
PP-c	280,000	5.3	2.1	37

EXPERIMENTAL

Materials

The three different molecular weight (M_w) of injection-molded PP; PP-a, PP-b, and PP-c, were supplied by the Japan Polypropylene Corporation. Melt flow rate (MFR), tensile modulus, and tensile yield stress are shown in Table I. The dimensions of the injection-molded samples were measured as 120 × 120 × 3 mm^3.

Microcutting test

Surface mechanical property of materials in terms of shear strength distribution near the surface was measured by using a surface/interface mechanical testing machine [Surface and interface cutting analysis system (SAICAS) model DN-20S; DAIPLA Wintes Co.]. Figure 1 shows the schematic diagram of the cutting process. The microcutting test was conducted with a constant speed mode. It should be noted that the depth of cutting process is not constant but increases as the cutting tool moved.[31] A diamond blade with 0.5-mm width was used to perform the test; the vertical speed and horizontal speed were set at 2 and 0.2 μm/s, respectively. The observation area was cut along the injection flow direction (FD). The shear strength distribution near the surface can be calculated with measuring the horizontal force reaction during cutting the surface of specimen, as shown in Figure 1, by using the following equation[32]:

$$\text{Shear strength}(\tau) = \frac{F_H}{2 \times W \times d \times \cot\theta} \quad (1)$$

where F_H is the horizontal force, W is the width of the blade, d is the depth of the cut, and θ is the shear angle. Note that the shear angle (θ) can be obtained by using the following equation[31]:

$$\theta = \frac{\pi}{4} - \frac{1}{2}\arctan\left(\frac{F_v}{F_h}\right) \quad (2)$$

where F_h and F_v are force component parallel and perpendicular to the surface, respectively. Note that this relation, first obtained by Merchant.[33]

Scratch test

A scratch machine model KK-01 (KATO Tech Co.) was used to perform the progressive load scratch test according to ISO 19252, in this study. A linearly load increasing test of 1–50 N with different constant scratch velocities at 1, 10, 100, and 200 mm/s was conducted. The scratch length for each scratch test was fixed at 100 mm. A stainless steel spherical scratch tip with 1 mm in diameter was used and the tests were performed at room temperature. The scratch direction was parallel to the injection flow line to prevent variation in scratch damage due to possible orientation effects.[18] The obtained values are the averaged of three specimens for each condition.

Scratched surface observation

A commercial scanner model EPSON GT-X970 Photo PC was used to scan the scratched surfaces at a resolution of 3200 × 3200 dpi in eight-bit grayscale level. A threshold function in ImageJ software was adapted to scanned images for evaluating the scratched damage transitions.[34]

Subsurface observation

To investigate the relationship between scratch behavior and the damage deformation under scratched surface especially at the onset of scratch visibility, a thin cross-section of scratched samples was observed by POM. A scratched sample was cut along the transverse directions to the scratch line

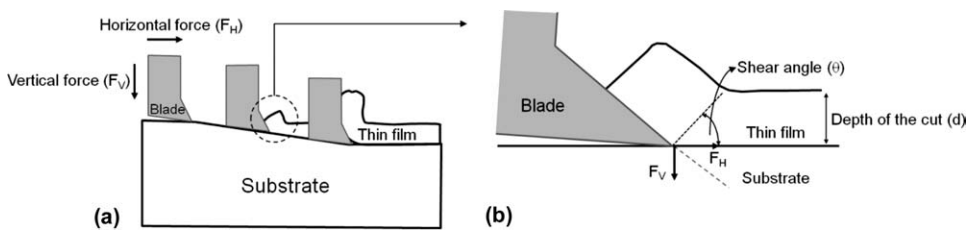

Figure 1 (a) Schematic diagram of the cutting process and (b) schematic diagram enlarged at the cutting portion shows the reaction forces.

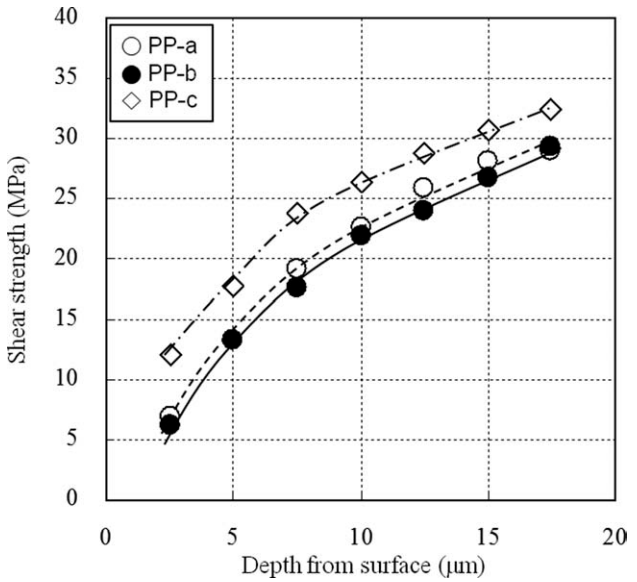

Figure 2 Shear strength near the surface for three different PP systems. The observation direction is in FD.

(TD cross-section) and molded with epoxy resin. The sample then was carefully polished after that attached on a glass slide. The remaining sample was polished to a thickness of ~30 μm. Sample was then polished by using Al_2O_3 aqueous emulsion. The polarized optical microscope (Nikon ECLIPSE model E600 POL) was used in transmission mode to observe damage transitions on the sample surface.

RESULTS AND DISCUSSION

Material characteristics

Tensile properties of three PP systems are summarized in Table I. The three systems exhibit similar tensile yield strength, however, PP-c shows higher tensile modulus compared with the other two systems. This is due to the fact that the bulk mechanical properties of the polymer can be enhanced by increasing M_w. Generally, the injection-molded parts exhibit an inhomogeneous structure, namely a skin-core structure.[35,36] It has been reported that the skin-layer thickness increases as the M_w increased.[18,36] In injection-molded polymers, the scratch performance is more significantly affected by the skin instead of the core.[13] Therefore, the surface mechanical property evaluated by microcutting method must be considered as an important parameter for describing the scratch properties. The values of shear strength distribution near the surface for the three PP systems calculated using eq. (1) are shown in Figure 2. The shear strength near the surface of PP-c was higher than that of PP-a and PP-b. The result suggested that increasing M_w has been shown to be effective in enhancing both bulk mechanical properties and also surface mechanical property.

Scratch behavior

Surface scratched damage modes in TPO scratched under progressive load have been reported.[18–20,37] The three regions of typical surface damage in scratched PP were reported to be observed, i.e. mar, fish-scale, and material removal or cutting. The damage mode in the first region is term "mar" where the tip causes a smooth, compressive-type indentation that slightly scatters light and alters the local surface gloss. Further increase scratch load (region 2), the scratch tip pulls the material underneath in a ductile manner without rupturing the surface. At this point, a parabolic pattern called "fish-scale" takes place within the scratch groove. This pattern will become large enough to scatter light and lead to scratch visibility. An onset of scratch visibility or onset of whitening is where the scratched damage can be detected by necked eyes due to the increase in whiteness of the scratch groove. As the scratch load continues increasing, the severe damage can be observed in region 3. Material removal zone or cutting pattern is where the scratch tip penetrates through the top surface and begins to displace the material around it. In this study, these scratch damage modes were observed and chosen as criteria to evaluate scratch behavior of PP. Figure 3 shows scanned images and images from gray scale threshold function in Image-J program analysis. The PP-a system was chosen as a model system to study the effect of scratch velocity on scratch behavior. It can be clearly seen from Figure 3 that the scratch velocity increased from 1 to 200 mm/s, the onset of scratch visibility, which indicated by the arrows, appears to occur earlier. A similar observation in a compression-molded TPO for the onset of scratch

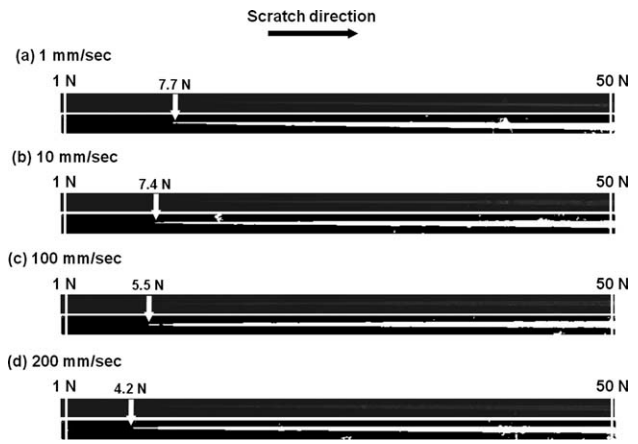

Figure 3 Scanned images and treated images of scratch test on PP-a system with different constant scratch velocities at (a) 1, (b) 10, (c) 100, and (d) 200 mm/s.

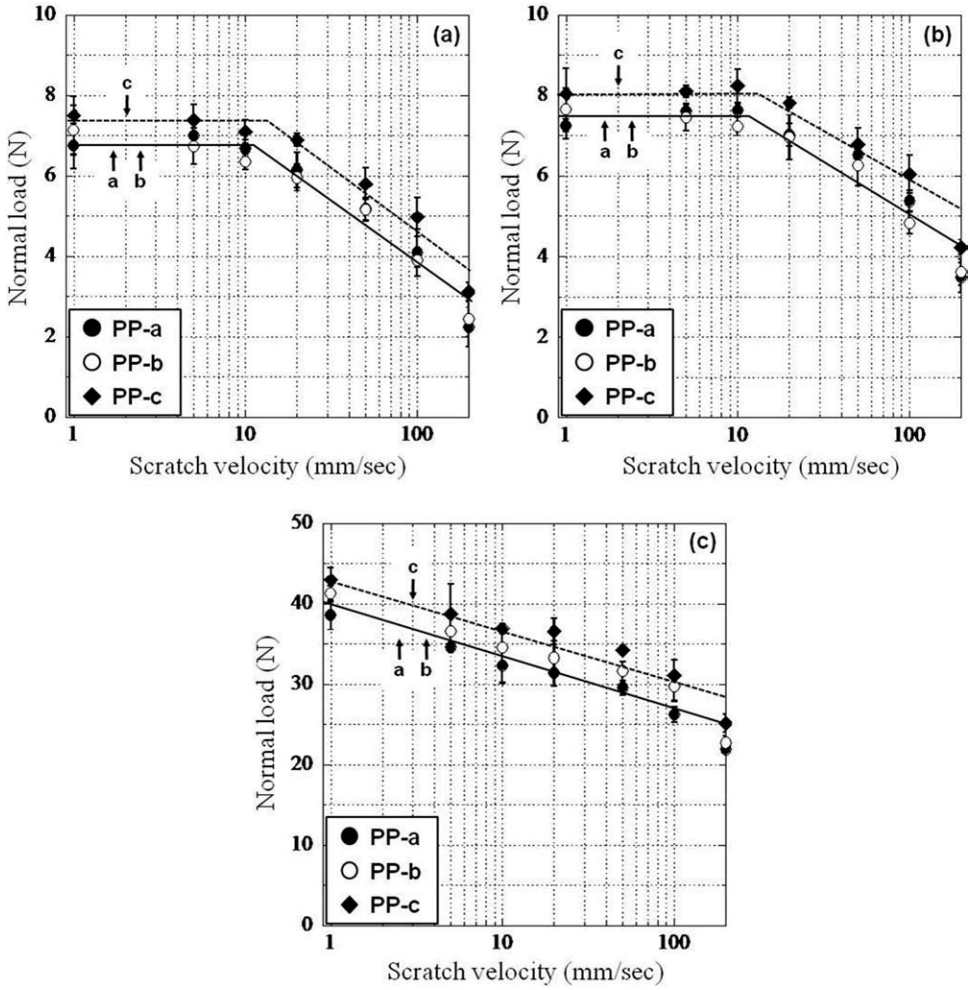

Figure 4 Critical normal load as a function of scratch velocity for comparing three different PP systems: (a) transition to fish-scale, (b) onset of scratch visibility, and (c) transition to cutting.

visibility was reported by Browning et al.[19] The relationships between critical normal load for each scratch damage transition and scratch velocities are shown in Figure 4, such as fish-scale, visibility, and cutting. The solid line represents typical trend of scratch velocity on scratch behavior observed for PP-a, the rest of samples are also showed in the similar trend. The critical normal load for transition to fish-scale pattern and onset of scratch visibility was not affected by scratch velocity in the range of 1–10 mm/s. However, the critical normal load significantly decreased when the scratch velocity was higher than 10 mm/s. Whereas critical normal load for transition to cutting is linearly decreased as increased scratch velocity [Fig. 4(c)]. However, the trend of the scratch velocity effect on cutting pattern is different from fish-scale and visibility. The above results are correlated to the scratch coefficient of friction (SCOF) (Fig. 5). The SCOF is defined as the ratio of the tangential force to the normal force.[34] Consider the scratch distance from 0 to 20 mm, the SCOF for the low-scratch velocities (1 and 10 mm/s) is lower than that of the high-scratch velocities (100 and 200 mm/s). The trend indicates that higher SCOF results in lower critical normal load for scratch damage transition especially for onset of

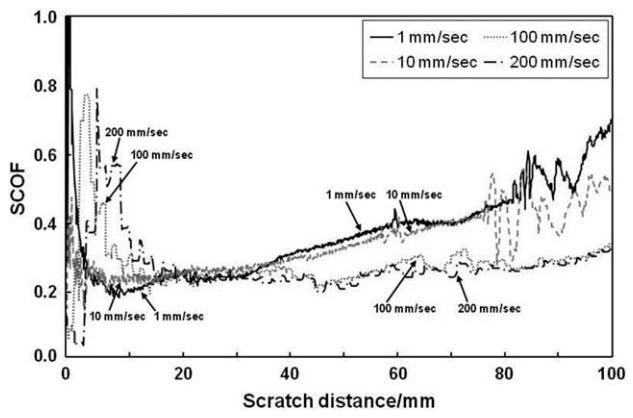

Figure 5 Comparison of SCOF curves of PP-a system scratched with different constant scratch velocities at 1, 10, 100, and 200 mm/s.

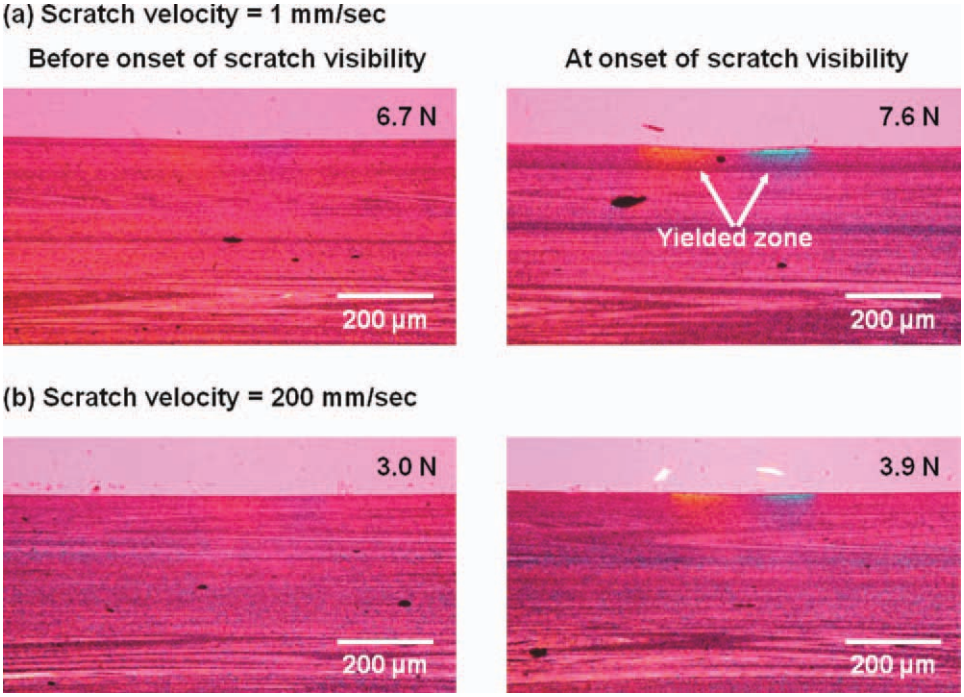

Figure 6 POM micrographs of TD cross-section subsurface deformation for PP-a system after scratched under progressive load test with different constant scratch velocities at (a) 1 and (b) 200 mm/s. [Color figure can be viewed in the online issue, which is available at wileyonlinelibrary.com.]

scratch visibility. It can be seen that the SCOF of low-scratch velocities increases gradually with the increase of scratch distance. This increment is due to scratch tip penetrated through the substrate deeper with low-scratch velocities. However, the SCOF of high-scratch velocities does not change appreciably. The similar SCOF curves have been observed in PP-b and PP-c.

Subsurface observation

The scratch damage mechanism at onset of scratch visibility of PP has not been clearly investigated yet. To understand this mechanism, the subsurface analysis by POM was examined. POM micrographs of PP-a system in TD cross-section scratched at scratch velocity of 1 and 200 mm/s are shown in Figure 6. At the onset of scratch visibility in both cases, a radial birefringent zone was clearly observed on the subsurface while it was not observed before onset of scratch visibility. This birefringent zone is observed due to yielding behavior of polymers, and it can be implied that scratch damage deformation mode changes from elastic deformation to plastic deformation. Hence, it was proven that yield behavior in the subsurface is correlated to the onset of scratch visibility. Moreover, the yielded zone size of high-scratch velocity is smaller than that of low-scratch velocity. The effect of scratch velocity on the yielded zone size is clearly observed in Figure 7. These micrographs were taken at the onset of cutting pattern. It was found that the yielded zone size under scratched groove becomes shallower and formed near the surface at 200 mm/s. The depth of yielded zone formed at scratch velocity of 1 mm/s is around

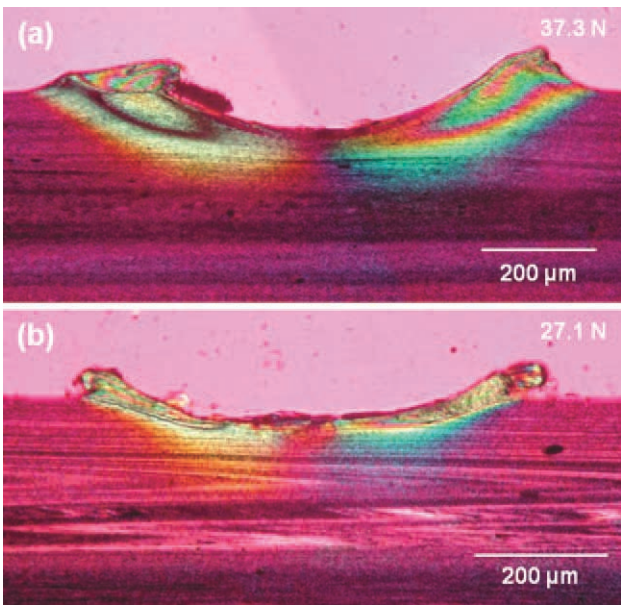

Figure 7 POM micrographs of TD cross-section at onset of cutting pattern of PP-a system after scratched under progressive load test with different constant scratch velocities at (a) 1 and (b) 200 mm/s. [Color figure can be viewed in the online issue, which is available at wileyonlinelibrary.com.]

160 μm and that at 200 mm/s is around 80 μm. This result indicated that localized stress was generated near the surface at higher scratch velocity.

This study clearly shows that scratch behavior of polymer materials is strongly rate-dependent. As the similar results have been observed in PP-b and PP-c, these results are also quantitatively reported in Figure 4. The result shows that PP-c with the lowest MFR tends to promote better scratch resistance. This might be due to the highest tensile properties and shear strength near the surface as shown in Table I and Figure 2, respectively.

CONCLUSION

The effect of scratch velocity on scratch behavior of injection-molded PP was studied using the progressive load scratch test according to ISO 19252. The critical normal loads for the onset of scratch visibility, transitions to fish-scale pattern and cutting pattern decreased with increasing scratch velocity. The subsurface deformation shows that the yielded zone becomes shallower at a high-scratch velocity. Thus, localized stress was generated near the surface at a high-scratch velocity. It was found that the onset of scratch visibility, i.e. the formation of visible scratch damage, is correlated to yielding behavior of the subsurface under scratch loading.

The authors acknowledge the material support provided by the Japan Polypropylene Corporation. They thank Mr. Mikihiko Fujiwara of Japan Polypropylene Corporation for his support and assistance in this study.

References

1. Jiang, H.; Browning, R.; Sue H.-J. Polymer 2009, 50, 4056.
2. Jiang, H.; Browning, R. L.; Hossain, M. M.; Sue, H.-J.; Fujiwara, M. Appl Surf Sci 2010, 256, 6324.
3. Xiang, C.; Sue, H.-J.; Chu, J.; Masuda, K. Polym Eng Sci 2001, 41, 23.
4. Dasari, A.; Rohrmann, J.; Misra, R. D. K. Macromol Mater Eng 2002, 287, 889.
5. Misra, R. D. K.; Hadal, R.; Duncan, S. J. Acta Mater 2004, 52, 4363.
6. Xiang, C.; Sue, H.-J.; Chu, J.; Coleman, B. J Polym Sci Part B: Polym Phys 2001, 39, 47.
7. Lim, G. T.; Wong, M.-H.; Reddy, J. N.; Sue, H.-J. J Coat Technol Res 2005, 2, 361.
8. Tabor, D. The Hardness of Metals; Oxford University Press: Oxford, 1951.
9. Bowden, F. P.; Tabor, D. The Friction and Lubrication of Solids Part II; Oxford University Press: Oxford, 1964.
10. Guevin, P. R. J. J Coat Technol 1995, 67, 61.
11. Chen, Z.; Wu, L. Y. L.; Chwa, E.; Tham, O. Mater Sci Eng A 2008, 493, 292.
12. Chu, J.; Rumao, L.; Coleman, B. Polym Eng Sci 1998, 38, 1906.
13. Chu, J.; Xiang, C.; Sue, H.-J.; Hollis, R. D. Polym Eng Sci 2000, 40, 944.
14. Wong, M.; Lim, G. T.; Moyse, A.; Reddy, J. N.; Sue. H.-J. Wear 2004, 256, 1214.
15. Wong, M.; Moyse, A.; Lee, F.; Sue, H.-J. J Mater Sci 2004, 39, 3239.
16. ASTM International, ASTM D7027-05, Annual Book of ASTM Standards, 2005.
17. ISO 19252, International Organization of Standardization, 2008.
18. Moghbelli, E.; Browning, R. L.; Boo, W.-J.; Hahn, S. F., Feick, L. J. E.; Sue, H.-J. Tribol Int 2008, 41, 425.
19. Browning, R. L.; Jiang, H.; Moyse, A.; Sue, H.-J.; Iseki, Y.; Ohtani, K.; Ijichi, Y. J Mater Sci 2008, 43, 1357.
20. Jiang, H.; Browing, R.; Fincher, J.; Gasbarro, A.; Jones, S.; Sue, H.-J. Appl Surf Sci 2008, 254, 4494.
21. Hadal, S. K.; Misra, R. D. K. Mater Sci Eng A 2005, 398, 252.
22. Tang, H.; Martin D. C. J Mater Sci 2003, 38, 803.
23. Rongarajan, P.; Sinha, M.; Watkins, V.; Harding, K. Polym Eng Sci 2003, 43, 749.
24. Koch, T.; Machl, D. Polym Test 2007, 26, 927.
25. Briscoe, B. J.; Delfino, A.; Pelillo, E. Wear 1999, 225, 319.
26. Briscoe, B. J. Tribol Int 1998, 31, 121.
27. Briscoe, B. J.; Pelillo, E.; Sinha, S. K. Polym Eng Sci 1996, 36, 2996.
28. Briscoe, B. J.; Evans, P. D.; Pelillo, E.; Sinha, S. K. Wear 1996, 200, 137.
29. Briscoe, B. J.; Evans, P. D.; Biswas, S. K.; Sinha, S. K. Tribol Int 1996, 29, 93.
30. Briscoe, B. J.; Pelillo, E.; Ragazzi, F.; Sinha, S. K. Polymer 1998, 39, 2161.
31. Saito, F.; Nishiyama, I.; Hyodo, T. Mater Lett 2009, 63, 2257.
32. Iwamori, S.; Hasegawa, N.; Uemura, A.; Tanabe, T.; Nishiyama, I. Vacuum 2010, 84, 592.
33. Shaw, M. C. Metal Cutting Principles; Oxford Series on Advanced Manufacturing 3; Oxford Press: New York, 1984.
34. Browning, R.; Lim, G. T.; Moyse, A.; Sun, L.; Sue, H.-J. Polym Eng Sci 2006, 10, 601.
35. Zhong, G.-J.; Li, L.; Mendes, E.; Byelov, D.; Fu, Q.; Li, Z.-M. Macromolecules 2006, 39, 6771.
36. Wenig, W.; Stolzenberger, C. J Mater Sci 1996, 31, 2478.
37. Chu, J.; Xiang, C.; Sue, H.-J.; Hollis, R. Polym Eng Sci 2000, 40, 944.